Chapter 2

H I deficiency in X-ray bright groups - a statistical study

Gas deficiency in cluster spirals is well known and ram-pressure stripping is considered the main gas removal mechanism. In some compact groups too gas deficiency is reported. However, gas deficiency in loose groups is not yet well established. Lower dispersion of the member velocities and the lower density of the intra-group medium in small loose groups favour tidal stripping as the main gas removal process in them. Recent releases of data from H I Parkes all sky survey (HIPASS) and catalogues of nearby loose groups with associated diffuse X-ray emission have allowed us to test this notion ([8], [83]). In this chapter, we address the following questions: (a) do galaxies in groups with diffuse X-ray emission statistically have lower gas content compared to the ones in groups without diffuse X-ray emission? (b) does H I deficiency vary with the X-ray luminosity, L_x, of the loose group in a systematic way?

2.1 Introduction

In field galaxies, neutral hydrogen gas gets either converted into molecular form (and into stars) or ionised. A small fraction does escape in galactic winds. However in galaxies in clusters, substantial amount of gas goes into the intra-cluster medium (ICM), making the members *deficient* in H I relative to the gas content of a field galaxy of a similar morphological type. Such H I deficiency in cluster spirals is well reported in the literature. Members in groups may also lose gas to the intra-group medium (IGM) and become relatively *deficient* in H I. Galaxies in some of the Hickson compact groups have been reported to be gas deficient [155] but such deficiency is still debated [136]. Gas deficiency in loose group environment has not yet been investigated systematically. For the first time, H I deficiency by a factor more than 1.6 has been reported in some members of a non-compact group in the Puppis region [29]. In some of the loose groups, the IGM is found to have enhanced metalicity, suggesting recent gas removal from the member galaxies [39]. Thus, investigating gas removal processes operating in loose groups is timely and important.

Two mechanisms are considered important for gas removal: tidal interaction and ram-pressure stripping. Ram pressure stripping [58] is effective when the H I surface mass density is less than $\rho_0 v^2/(2\pi\, G\sigma_*)$, where σ_* is the stellar surface mass density. Clearly, larger the ICM or IGM density, ρ_0, and galaxy velocity dispersion, v, the more effective is this stripping. Clusters satisfy these requirements and ram-pressure stripping is considered an effective process in them. In groups, though, both these quantities are lower, especially dispersion by a factor of 10 and therefore ram pressure stripping is considered ineffective. Tidal interactions on the other hand, involve gravitational interaction between two or more galaxies as they pass by each other. The lower relative velocities in groups allow larger interaction timescales making tidal stripping the likely process for gas removal. This, in a larger sense, includes galaxy 'harassment', where the tidal stripping is caused by the overall gravitational potential of the group. However, a significant number of loose groups have been found to have hot gas in them emitting diffuse X-rays [97]. In such cases, ram pressure assistance

cannot be ruled out, making X-ray bright groups more H I deficient than non X-ray bright groups.

Chamaraux & Masnou (2004) [29] studied selected galaxies in five groups, NGC 533, 5044, 2300, 5846 and 4261, detected to have a hot IGM by ROSAT, and found a few of them to be strongly deficient in H I. They find the deficiency to be related to the physical proximity of the galaxy to the X-ray region. We have undertaken to study in detail the H I content of galaxies in groups with and without X-ray detection, covering a wide-range in X-ray luminosity. Here we report the first part of our study, viz. a comparative analysis of H I content in small loose groups based on HIPASS and other existing single dish data. The chapter is organised as follows: the next section deals with the sample selection, H I data and its processing details. In Section 3, we report the analyses of the data and our results. The possible explanations of the results are discussed in Section 4. The work is summarised in Section 5.

2.2 Sample, Data & Processing

Our sample is made of twenty seven groups, ten belonging to the X-ray bright category and seventeen belonging to the non X-ray bright category. We chose all the X-ray bright groups, totalling 10, from the X-ray atlas of nearby poor groups [97] satisfying the following criteria: most members have single dish H I measurements, their distances < 50 Mpc (a value of 100 km s^{-1} Mpc^{-1} is used for the Hubble constant throughout this work) and their membership is less than 25 (a convinient number we adopted to avoid poor clusters). Their X-ray luminosities are in the range from 2.0 $\times 10^{40}$ and 6.3 $\times 10^{42}$ erg s^{-1}. Eight X-ray non-detected groups (six from [97], and two from [104]) and 9 all-spiral groups (all the group members being late type spirals), make up the non X-ray bright category. Non compact all spiral groups are not expected to have diffuse X-rays from their IGM ([97], [62], [106], [104]) and therefore have been included to augment the non X-ray bright sample. The distances and memberships of these seventeen groups also follow the same criteria as the X-ray bright groups.

Among the 27 groups that make up our sample, 13 are from the southern hemisphere and 14 are from the northern hemisphere. For most of the southern hemisphere galaxies HIPASS database has been used. Given that typical H I masses in these galaxies will be a few times 10^8 $M_\odot$, the HIPASS sensitivity constrains that these groups be nearer than $\sim$ 40 Mpc. For the rest of the galaxies, H I measurements from the literature have been used ([68], [40], [54], [60], [87], [88], [124], [123], [142]). This imposes some practical difficulties: different surveys have different detection limits and resolution; some of the group members did not have any H I observation; in some other cases, the errors on the integrated flux densities were not quoted and we have used an average of the errors quoted for the other group members.

For group memberships we have followed the Lyon Group of Galaxies (LGG) catalog [48]. All LGG members of a group within a diameter of 1.2 Mpc (typical crossing distance in $\sim$ 5 Gyr) about the group center are included. In most cases, this circle seems a natural boundary. In a few cases where a significant fraction of LGG members lie outside this range, we have extended the circle to a diameter of 1.5 Mpc about the group center. This is done to ensure that the computed H I deficiency truely reflects the property of the group. Galaxies lying outside a diameter of 1.5 Mpc have been excluded. We also include as members of the group all galaxies found using NASA Extragalactic Database (NED) within the spatial and velocity extent defined by the LGG members. All members thus chosen are tabulated in Tables 3 and 4 under their respective group names with distances to the groups derived from their velocities given in brackets. The table lists the source names, morphological type (*MT*), optical diameter in arcminute ($d_l(')$), gas surface matter density in logarithmic units (*SMD*), H I deficiency ($def_{\rm H_I}$), angular distance from the group centre in arcmin (Ang.) and the telescopes used for obtaining the H I data (Tel.). Footnote at the end of Table 4 explains the symbols used for the different telescopes. Groups have been ordered in increasing right ascension but the galaxies within the groups have been ordered in increasing distance from their centers. The later ordering has been done to highlight the location of early-type and H I deficient galaxies with respect to the group centers. For galaxies that belong to an early morphological type (E,S0 and S0/a), a "–" is marked in columns 4, 5 and 7; such galaxies

have not been used in this study. Spiral galaxies which do not have H I data are denoted by an "X" in column 7. A "ND" in column 7 indicates a spiral not detected in H I. Optical diameter, d_l, is taken from RC3 catalogue using NED: it is the optical major isophotal diameter measured at or reduced to a surface brightness level $m_B = 25.0$ B-m/ss.

The HIPASS spectra obtained towards the galaxies were used to find the centroid velocities and the integrated flux densities ($\int S\,dV$ in Jy km s^{-1}, S being the flux per beam per channel and dV being the velocity resolution) after fitting and removing second order polynomial baselines. Unipops package was used for this processing. Errors on the integrated flux densitites were estimated as a product of the channel width of the HIPASS spectra, the channel rms and the square root of the number of channels occupied by the line.

There were several instances of confusion in the case of HIPASS data (Parkes beam has an FWHM of 15.5' at 21 cm). In the case of northern groups, multiple measurements with different telescopes were available. This and the fact that the beamsizes were smaller than that of Parkes reduced the instances of confusion. In all cases of confusion, the deficiencies have been calculated assuming it to be equal among the confused galaxies.

The total gas mass ($M_{\rm H_I}$) can not be straight away used for studying gas removal in galaxies as the H I content depends both on their sizes and morphological types. In fact, the disk size seems to be a more important diagnostic for the H I mass than the morphological type [59]. Gas mass surface density $M_{\rm H_I}/D_l^2$ proves to be a better measure of H I content as it incorporates the diameter of the spiral disk. Another advantage of using $M_{\rm H_I}/D_l^2$ over $M_{\rm H_I}$ as a measure of H I content is that $M_{\rm H_I}/D_l^2$ is distance independent and therefore free from its uncertainty.

The expected values of $M_{\rm H_I}/D_l^2$ for various morphological types are taken from [59]. While [59] used the UGC blue major diameters, we have used the RC3 major diameters. To take care of the difference in the surface matter densities that result from the use of RC3 diameters, we add a value of 0.08 [51] to the expected surface matter densities given by [59]. The final values of expected $M_{\rm H_I}/D_l^2$ used in this work are given in Table 1. H I deficiency of a single

Table 2.1: Expected surface matter densities for different morphological types (adapted from [59] for using RC3 diameters instead of UGC diameters.

Morphological (*M.T.*) &	type Index	$\log(\frac{M_{H_I}/D_l^2}{M_\odot/kpc^2})_{pred}$ ± s.d
Sa,Sab	2	6.77 ± 0.32
Sb	3	6.91 ± 0.26
Sbc	4	6.93 ± 0.19
Sc	5	6.87 ± 0.19
Scd,Sd,Irr,Sm,Sdm, dSp	6	6.95 ± 0.17
Pec	7	7.14 ± 0.28

galaxy is determined following the usual definition viz.:

$$def_{\rm H\,I} = log\frac{M_{H_I}}{D_l^2}|_{pred} \; - \; log\frac{M_{H_I}}{D_l^2}|_{obs} \tag{2.1}$$

An average of this over all the H I detected galaxies is used as a measure of the H I deficiency of the groups, hereafter referred to as the "group deficiency". Table 2 lists the group names, their X-ray luminosity in logarithmic units, the calculated group deficiencies with 1 σ error on them, for the 10 X-ray bright groups, the 8 X-ray non-detected ones and the 9 all-spiral groups that have no reported X-ray observation.

This way of accessing H I deficiency of a galaxy has some limitations. The scatter in the field H I surface density values ([59]) restricts us most often to unambiguously estimate the deficiency of a galaxy. For example, galaxies which have lost about half their gas content, cannot be termed H I deficient with certainty because of this reason. Thus in this work, the average deficiency of a large number of galaxies ("group deficiency"), has been used to find if X-ray bright groups are more H I deficient. Also the sample of field galaxies consists of many bright nearby galaxies and is known to suffer from Malmquist bias. However, according to the authors ([59]), this sample contains a healthy population of distant objects and is therefore suitable for comparison with galaxies of similar optical properties at relatively large distances.

Table 2.2: Estimated group deficiencies

Group Name	L_x, erg s^{-1}	Group deficiency
NGC524	40.53	0.62 ± 0.240
NGC720	40.86	0.42 ± 0.138
NGC1589 (NGC1587)	40.92	0.46 ± 0.157
NGC3686 (NGC3607)	40.53	0.07 ± 0.062
NGC4261	41.89	0.16 ± 0.134
NGC4589 (NGC4291)	40.74	0.12 ± 0.062
NGC5044	42.81	0.34 ± 0.082
UGC12064	42.17	0.06 ± 0.055
IC1459	40.52	0.29 ± 0.093
NGC7619	42.05	0.20 ± 0.053
NGC584	<40.51	0.36 ± 0.063
NGC1792 (NGC1808)	<39.79	0.20 ± 0.059
NGC5061 (NGC5101)	<40.77	0.08 ± 0.102
NGC5907 (NGC5866)	<39.48	-0.08 ±0.174
UGC9858 (NGC5929)	<40.50	0.39 ±0.055
NGC7448	<40.40	-0.11 ±0.050
NGC7582	<40.74	0.27 ± 0.055
NGC7716 (NGC7714)	<39.72	0.22 ± 0.032
NGC628	no observation	-0.20 ±0.154
NGC841	no observation	0.14 ±0.088
IC1954	no observation	0.20 ± 0.108
NGC1519	no observation	0.24 ± 0.093
NGC2997	no observation	0.10 ± 0.050
NGC3264	no observation	-0.16 ±0.060
NGC4487	no observation	0.19 ± 0.104
NGC6949	no observation	-0.16 ±0.139
UGC12843	no observation	-0.05 ±0.115

Note: The group names given are from LGG catalogue. Those given in brackets are from [97] and [104].

2.3 H I content in galaxies in groups with and without diffuse X-ray emission

Both local and large scale environments affect the H I content in galaxies. Interactions and mergers are processes that are likely to be similar in groups with and without diffuse X-ray emission. Therefore, we first tested if the presence of diffuse X-ray gas affects the H I content any further. We find that, on average, the galaxies in X-ray groups have a H I deficiency of 0.28 ±0.04 whereas the ones in the non X-ray groups show an insignificant deficiency of 0.09 ±0.03. A few groups in the later catagory, eg. NGC584, NGC7582 and UGC9858, that have significant H I deficiency also have upper limits to their X-ray luminosities close to the lowest luminosity among the X-ray detected groups.

For the purpose of this analysis, we constituted two *composite* groups, one with and another without diffuse X-ray emission, using all the H I detected group members. The group distances are derived from the mean radial velocities of the H I detected members. These are used to convert the projected angular distances of the group members with respect to group centres to linear distances and the optical major diameters, d_l, to linear sizes. The top panel of Fig. 1 shows H I deficiency, as defined in section 2, for all members of these *composite* groups with respect to their radial distances. The same plot for the X-ray bright and non X-ray category have been shown separately in Figs. 2 and 3. Straight lines have been fitted through the data and the slopes show that the variation of H I deficiency with radial distance from the group centre is more prominent in X-ray bright groups than in non-Xray groups. The fractional number of H I deficient galaxies in X-ray groups is also higher than in non X-ray groups. The bottom panel of Fig. 1 shows H I deficiency distributed with respect to the linear sizes of the galaxies. H I deficiency seems to increase with size which could be a bias. $M_{\rm H_I}$ is observed to be proportional to $D_l^{1.7}$ [59]. Thus H I surface density decreases with D_l as $D_l^{0.3}$. So computing H I deficiency with a constant value of $M_{\rm H_I}/D_l^2$ for each type leads to an overestimate for galaxies of large diameters and an underestimate for those with small ones. The effect present in Fig. 1 agrees quantitatively with this explanation. The average

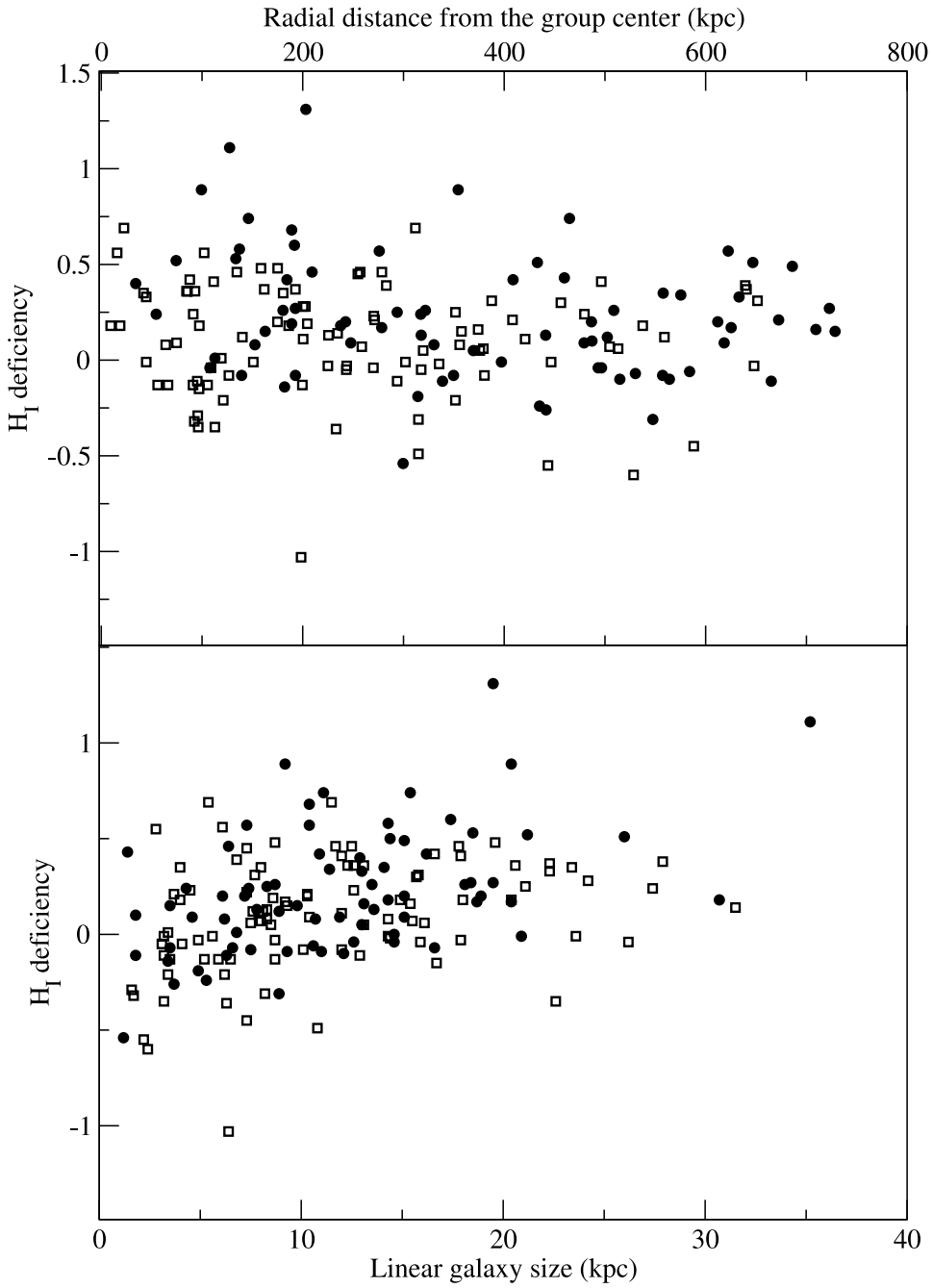

Figure 2.1: The top panel shows the distribution of H I deficiency with respect to the distance from the group centre. The bottom panel shows the distribution of H I deficiency with respect to the linear sizes of the galaxies. The number of galaxies in groups with and without Xray emission are 74 and 96, respectively.

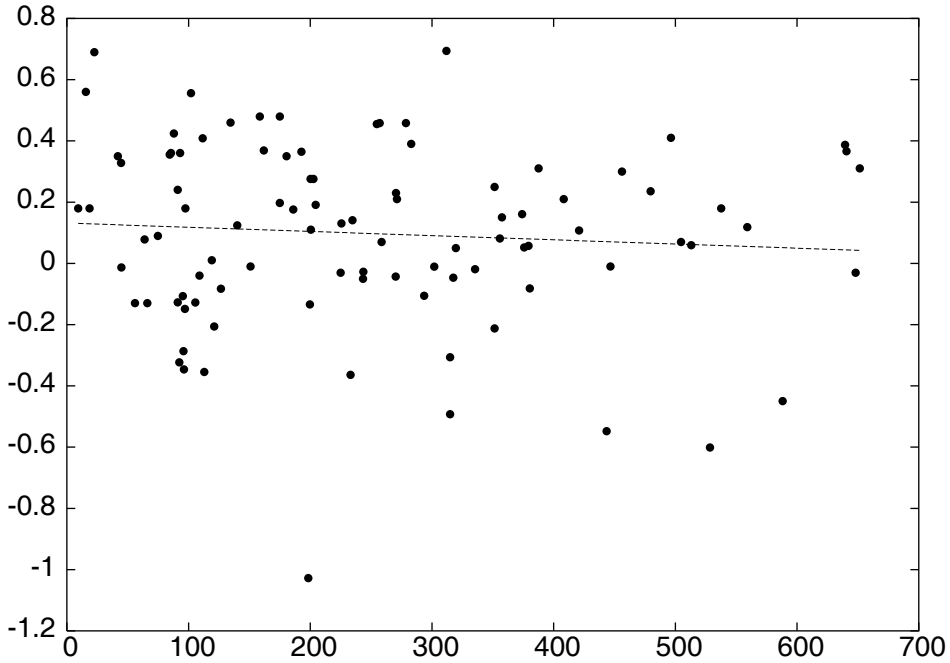

Figure 2.2: Plot of H I deficiency against projected radial distance (kpc) from the group centre, in non X-ray bright groups. The straight line is a fit to the data.

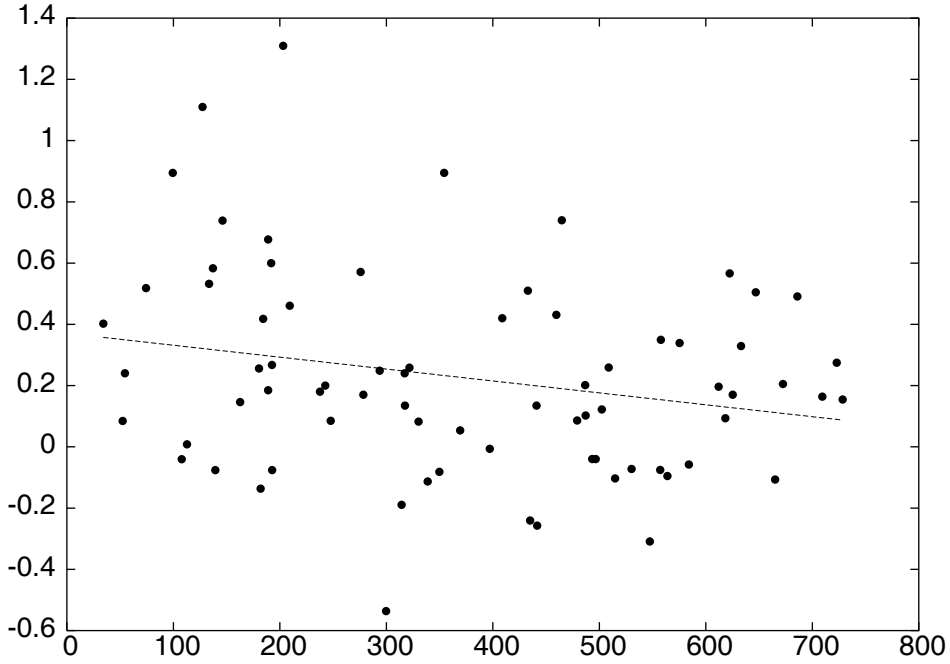

Figure 2.3: Plot of H I deficiency against projected distance (kpc) from the group centre, in X-ray bright groups. The straight line is a fit to the data.

effect of such a bias on the galaxies of the sample leads to an underestimate of 0.04 on $def_{\rm H\,I}$. However, this does not affect the results of our comparative study.

The top panel of Fig. 4 shows the cumulative distribution of H I deficiency for the two categories, Xray-bright and non X-ray groups. Cumulative distribution represents, for each value, q_i, of the quantity, q, given in the abscissae, the proportion of galaxies, for which $q < q_i$. Three statistical tests, Kolmogorov-Smirnov (KS), Mann-Whitney (MW) and Wald-Wolfowitz (WW), were performed on the cumulative distributions of the quantity to test if the two samples are drawn from the same parent population. In the case of H I deficiency the probabilities are: KS: 8.0%; MW: 6.0% and WW: 1.1%. The low probabilities indicate that the two groups are unlikely to be drawn from the same parent distribution, i.e. one group tends to be more H I rich relative to the other. The bottom panel of Fig. 4 shows the cumulative distribution of radial distances from the group center for the two categories, Xray-bright and non X-ray groups. The same three tests were performed on these distributions. Probabilities that the two composite groups are drawn from the same parent distribution from KS, MW and WW tests are 0.08, % 0.01% and 33.6%, respectively. Clearly, the X-ray bright groups are more extended compared to the non X-ray bright groups. The average radius of the X-ray bright groups is 600 kpc while that of the non X-ray bright groups is 475 kpc. Similarly, cumulative distribution functions for the optical surface brightness for the two composite groups (top pannel of Fig. 5) were constructed, to see if the process responsible for excess gas loss has also resulted in excess loss of stellar matter. In this case Wald-Wolfowitz Runs Test, Mann Whitney test and Kolmogorov Smirnov test returned a probability of 81%, 54% and 47%, respectively, showing that the two populations have same parent distribution. In other words, the two composite groups differ only in their gas content and therefore the IGM is likely to be responsible. The bottom pannel of Fig. 5, shows a comparison between the H I to optical flux ratio for the two groups, which reflects that the gas content in X-ray bright groups are comparatively less than in non X-ray groups. The cumulative distribution of X-ray bright group members saturate by the value of 6.75, whereas that of the non X-ray group members goes all the way upto 7.70. Small number statisitics, projection effects and

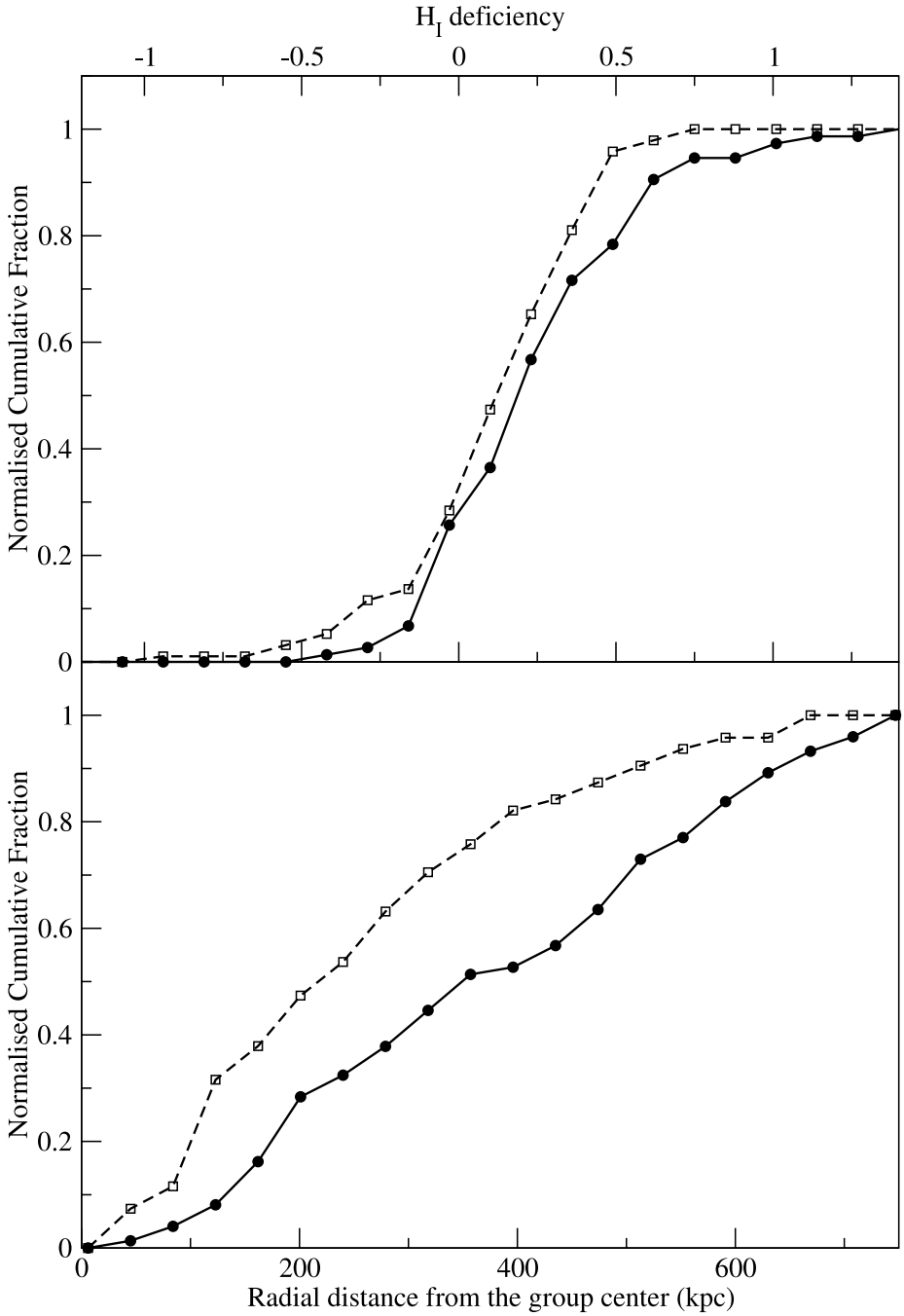

Figure 2.4: The top panel shows the behaviour of normalised cumulative fraction of the two sets of galaxies with respect to the H I deficiency; the bottom panel shows the same with respect to the radial distances from their group centres. Filled circles connected by solid lines represent galaxies in X-ray bright groups whereas empty squares connected by dashed lines represent galaxies in non X-ray groups

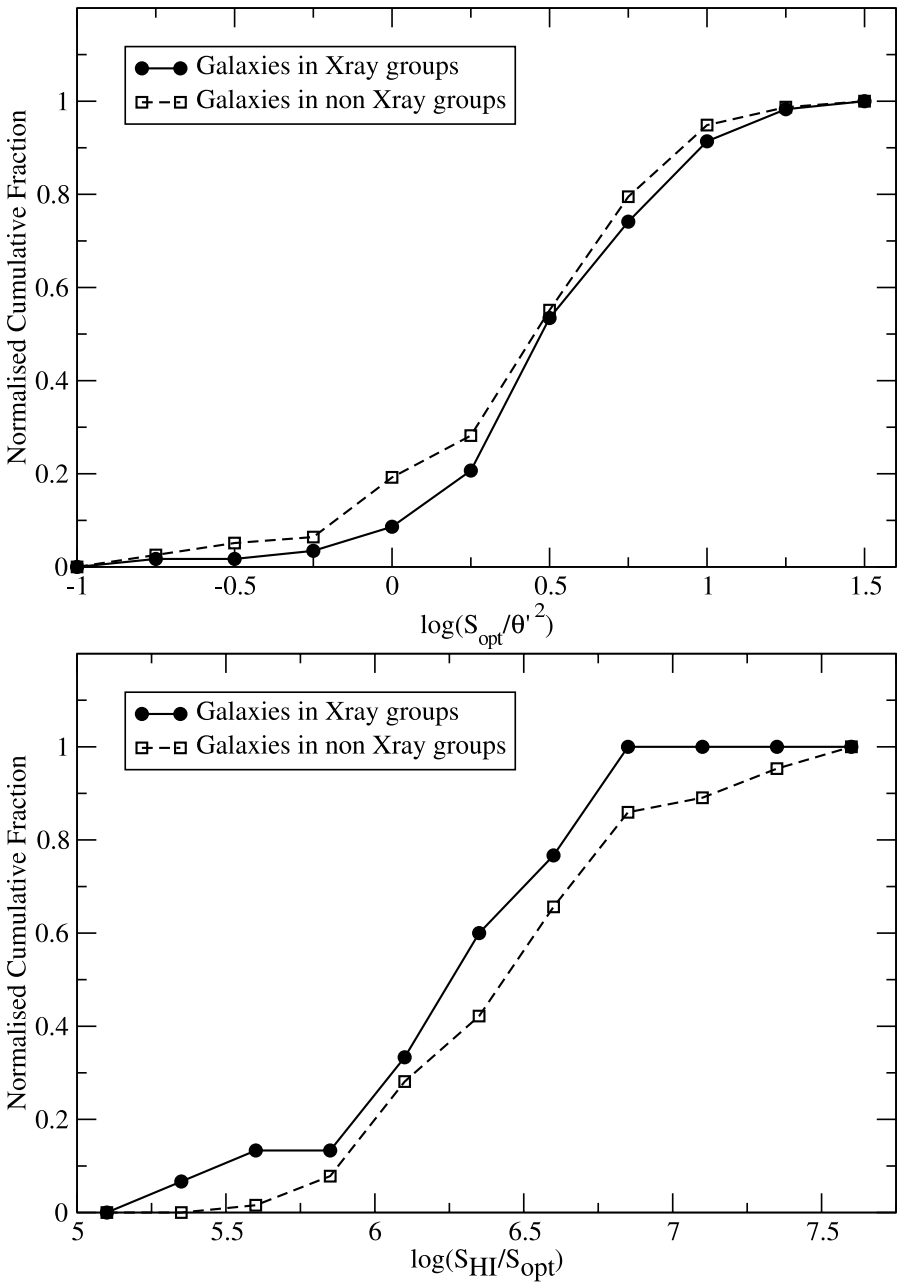

Figure 2.5: Comparison of optical and H I properties.

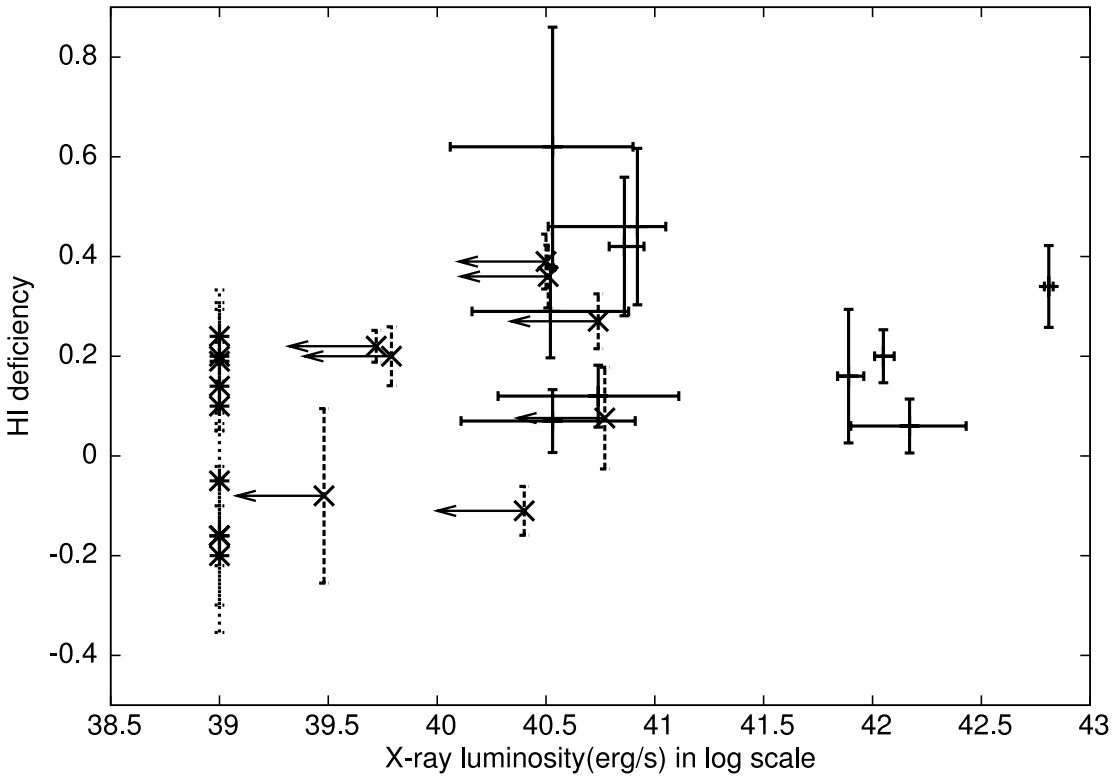

Figure 2.6: Variation in H I deficiency with L_x is shown.

distance uncertainties may still affect these results to some degree. Nonetheless, the above results support the premise that the galaxies in X-ray bright groups have statistically lower H I content and thereby higher H I deficiency compared to the ones in non X-ray groups.

Fig. 6 shows the plot of the group deficiency, as defined in section 2, against the X-ray luminosity (in log scale) of the studied groups. In this figure, the H I deficits of the nine all-spiral groups for which the X-ray luminosities are unknown, are marked at an X-ray luminosity ($erg\ s^{-1}$ in log scale) of 39.0. X-ray bright groups are represented with $\pm$ 1 σ errorbars on both X and Y values; X-ray non-detected groups having upper limits in X-ray luminosity are shown with arrows pointing to the left. No dependence with X-ray luminosity is seen, excepting that X-ray bright groups are deficient and non X-ray groups have near normal H I content.

The fraction of galaxies according to the morphological type index for the two categories are shown in Fig.7. As noted in other instances (Mulchaey *et al.* , 2003), we also find that the X-ray bright groups have a larger fraction of early type galaxies compared to non X-ray

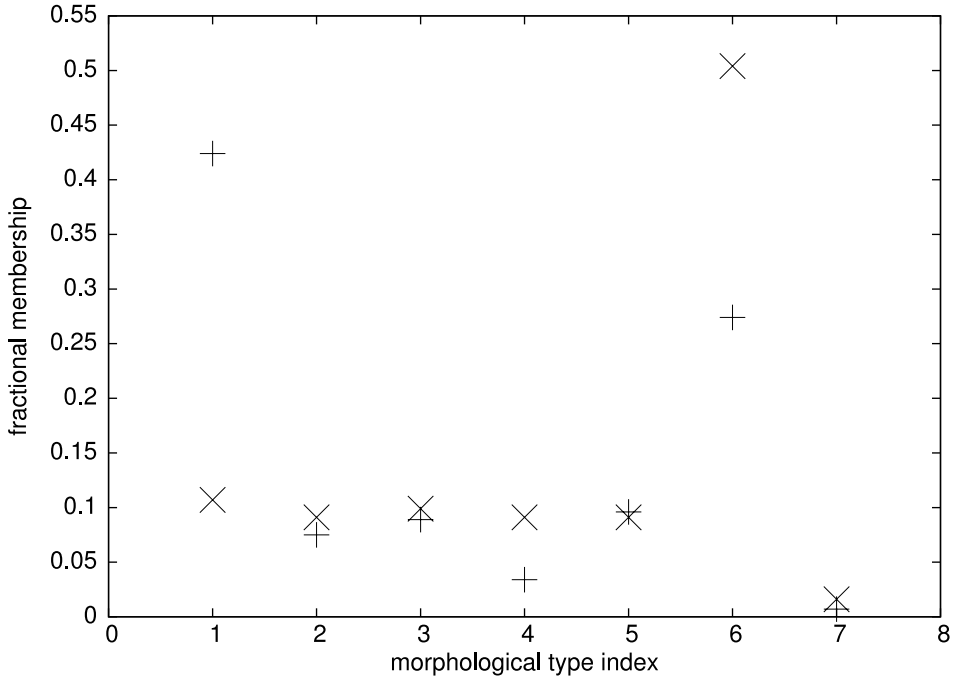

Figure 2.7: Distribution of galaxies from groups with and without diffuse X-ray emission with respect to morphological type index from Table 1 (here, Elliptical, S0 and S0/a types are grouped under index 1). Symbol '+' represent X-ray bright groups and 'x' represent non X-ray groups.

groups. Interestingly, the early type members are preferentially located close to the centers in the X-ray bright groups (Tables 3 & 4). Their exclusion in our analysis and the larger membership of the X-ray bright groups can possibly explain the finding that the X-ray bright groups are more extended than the non X-ray groups.

2.4 Discussion

Environment affects substantially the gas content, star formation rate and morphology of a galaxy as demonstrated by studies of cluster galaxies. Some observed properties of clusters viz. the population evolution with radius ie. from red, evolved and early type in the inner parts to bluer, younger and later type in the outer parts, the increase in the fraction of blue-galaxies (*Butcher-Oemler effect*; [20]) and decrease in the fraction of S0s (*morphological evolution*) with redshift, have led to considerations of mechanisms that change the star formation rate and morphology of cluster galaxies. Removal of the warm gas from the halo (*strangulation*) and the cold-gas from the disk (*ram pressure stripping* and *evaporation via*

thermal conduction) have been invoked to change the star formation rate. Major and minor mergers have been invoked to account for the *morphological evolution* (eg. [144], [101]). However, similarity in spectral and morphological properties of poor and more massive clusters at a redshift of ∼0.25 [6] and the level of suppression of star formation in galaxies in many clusters even at a radius of ∼1 Mpc are taken to imply *pre-processing* in *sub-clusters*: ie. some of the warm gas from the halo and the cold gas from disk seem to be lost in processes in less massive clusters at a higher redshift that merged to form today's rich clusters. *Strangulation, ram pressure* and *evaporation* seem to be playing a role in them [46].

Interactions and mergers are processes that are likely to be similar in groups with and without diffuse X-ray emission. Besides, tidal interactions are rare in group environments: for typical membership number (6 spirals), size (1.5 Mpc diameter) and dispersion (150 km/s) of a group, the number of encounters for 50% gas loss is 0.03 for the group (0.005 per spiral galaxy) in Hubble time [28]. Therefore, the amount of gas lost in this way seems insufficient to explain the observed group deficiencies in X-ray bright groups. However, our study suggests that processes such as *tidal aided ram pressure stripping* [39] and *evaporation via thermal conduction* may be effective even among present day loose groups. Our findings are: (a) the groups with diffuse X-ray emission seem to have lost more gas compared to groups without diffuse X-ray emission; (b) the X-ray bright groups are spatially more extended than the non X-ray groups. These findings indicate a role for the X-ray emitting gas in aiding H I removal from the galaxies.

In cluster environment ram pressure stripping has been seen to be an effective process for removing gas from galaxies. In groups this process was not considered to be an efficient one as lower IGM density and velocity dispersion, both smaller by an order of magnitude compared to clusters, make direct ram pressure stripping effective only below a critical H I column density of 10^{19} per cm^2 for a normal galaxy with an optical radius of 10 kpc, and 10^{11} stars . However in X-ray bright groups this picture can be a little different. From the quoted X-ray luminosity and temperature in [97],we have calculated the IGM densities assuming the emission to originate from thermal bremsstrahlung. The IGM densities thus calculated for

10 X-ray bright groups vary from 5×10^{-4} to 2×10^{-3} particles/cc. For a normal galaxy with an optical radius of 10 kpc and 10^{11} to 10^{10} stars, and for typical velocity dispersion quoted in the literature, the ram pressure effects become important at H I column densities $\sim 10^{19}$ to $\sim 10^{20}$ per cm^2. The range in stellar mass reflects the range in surface matter density. Ram pressure becomes effective even at higher H I column densities for low surface brightness galaxies. Low surface brightness galaxies do form a substantial fraction in groups. The velocity dispersion of galaxies in these groups are also not well determined. Recent discovery of several new members in NGC5044, an X-ray bright group, indicates that some of these groups can actually be more massive. In NGC5044, the new membership has increased its velocity dispersion from 119 km/s to 431 km/s [25]. For such a velocity dispersion and for a normal galaxy (with an optical radius of 10 kpc, and 10^{11} to 10^{10} stars), the ram pressure effects are significant at H I column densities of $\sim 5 \times 10^{19}$ to $\sim 5 \times 10^{20}$ per cm^2.

We have calculated the maximum gas loss possible through ram pressure alone for two galaxies in NGC 5044 group. We have assumed a velocity dispersion of 431 km/s and an IGM density of 0.0004 particles/cc. The later is about half the IGM density determined using X-ray data for this group [97]. We chose two galaxies differing in stellar mass by a factor of ten to determine the varying effects of ram pressure on different types of galaxies in a group. We determined their stellar masses using their J and K magnitudes [9]. In the first case of MCG-03-34-04, the stellar mass is found to be $\sim 1.5 \times 10^{10}$ $M_\odot$, and the corresponding critical H I column density beyond which the ram pressure can strip off gas is $\sim 4 \times 10^{19}$ per cm^2. For a gaussian distribution of H I [28] and using a peak column density of 3.2×10^{21} per cm^2 (from our interferometric data), it is seen that $\leq 5\%$ of the gas can be stripped off in this way. In the second case, MCG-03-34-041 is found to have a stellar content of $\sim 4 \times 10^9$ $M_\odot$ and a peak column density of 2.6×10^{21} per cm^2, leading to a gas loss of 32%.

Thus, ram pressure is probably an important gas removing mechanism in X-ray bright groups, either on its own or assisted by tidal interaction that stretches the gas below the critical column densities. However this is a density dependent mechanism and thus will be less efficient as the galaxy recedes the group centre, since the IGM density will decrease

with increasing distance from the centre. Also for groups with smaller velocity dispersion, this process will become much less effective as the ram pressure depends on the square of the velocity dispersion. For example, a galaxy like MCG-03-34-041 will lose only 5% gas if the velocity dispersion is 150 km/s. It may also be noted that for the ten X-ray bright groups for which we could determine the IGM densities (ρ), the quantity, $\rho\ \sigma_v^2$, is found to have no correlation with the group deficiency.

Evaporation via thermal conduction seems to be another process which can be responsible for mass loss from galaxies embedded in a hot medium [34]. It is interesting to note that *evaporation* depends directly on temperature and weakly on density, complementary to ram pressure processes. At temperature of $5\ \times\ 10^6$ K, typical of an X-ray bright group, a disk galaxy can loose as much as $4\ \times\ 10^7$ $M_\odot$ in the time it takes to cross the central 100 kpc region at 200 km/s speed. To expell a mass of 10^9 $M_\odot$ over a period of 10^9 years, it requires a mechanical power input of about $10^{39.5}$ $erg\ s^{-1}$, a fraction of the luminosity of the X-ray bright groups. This suggests that if a small fraction of the thermal energy in the hot gas is coupled to the galactic cold gas over a billion years, the gas in the outer parts of the galaxies can be stripped leading to the observed deficit in H I. The saturation of conductivity and effects of magnetic field may reduce this mass loss. However, mixing from gas-dynamic instabilities as the disk ploughs through the tenuous IGM may enhance the mass loss. Evaporation may also become *asymmetric* caused by the galaxy motion and the gradient in the temperature and density of the hot gas. Such asymmetric *evaporation* may further deposit momentum to the adjoining gas via (Spitzer's) rocket effect and enhance the gas loss. Numerical simulations of this process taking into account such effects may yield quantitative results and verify the viability of this mechanism. Such an attempt is beyond the scope of this work.

We plan to enlarge the data set by obtaining single dish data on more groups, with and without diffuse X-ray emission. This will help us to improve the confidence level in these results. We are also in the process of obtaining high resolution images of some members from both kinds of groups, looking for morphological evidence to try to pin down the responsible

process. Extended, asymmetric, low surface brightness H I distributions are typical signs of tidal interaction. Swept-back appearence of the H I gas along with the asymmetric structures, would suggest *tidal aided ram pressure stripping*. Evaporation will result in galaxies with somewhat smaller than usual H I diameters, and a depressed H I surface density across the entire face of the galaxy [22]. Thus, with sensitive synthesis data at moderate resolution, we hope to be able to assess the nature of gas removal and possibly conclude on the viable mechanism.

2.5 Conclusions

We have studied the H I content of galaxies in loose groups with and without diffuse X-ray emission. We find that the galaxies in non X-ray groups are not deficient in H I with respect to the field galaxies. The galaxies in X-ray groups are clearly deficient in H I and have lost more gas (H I) compared to those in non X-ray groups. No systematic dependence of the H I deficiency with L_x is found. We also find that the X-ray groups are more extended than non X-ray groups. *Tidal aided ram pressure stripping* and *evaporation* are the possible mechanisms leading to the excess gas loss found in galaxies in X-ray groups.

Table 2.3: Details of the galaxies in groups with diffuse X-ray emission

Galaxy	*MT*	$d_l(')$	*SMD*	$def_{\rm H_I}$	Ang.	Tel.
NGC524 (25.5 Mpc)						
NGC0524	S0	2.8	-	-	0.0	-
NGC0516	S0	1.4	-	-	9.8	-
NGC0518	Sa	1.7	6.81	−0.04	14.5	H
NGC0532	Sab	2.5	6.24	0.53	18.0	H
NGC0509	S0	1.6	-	-	21.6	-
IC0101	S?	1.4	6.23	0.68	25.4	A
NGC0522	Sc	2.63	5.56	1.31	27.4	A
IC0114	S0	1.7	-	-	32.3	-
CGCG411-038	S0	0.6	-	-	36.9	-
NGC0502	S0	1.1	-	-	40.4	-
NGC0489	S0	1.7	-	-	47.3	-
NGC 720 (16.6 Mpc)						
NGC720	E	4.7	-	-	0.0	-
2MASX-1[a]	S0	0.7	-	-	14.8	-
2MASX-2[b]	Sc	0.9	-	-	32.3	X
MCG-02-05-072	S0/a	1.3	-	-	34.4	-
KUG0147-138	Sb	1.5	6.70	0.20	50.2	H
DDO015	Sm	1.9	6.06	0.89	73.4	H
ARP004	Im	2.8	6.69	0.26	105.4	H
UGCA022	Sdm	2.7	6.62	0.33	131.1	H
NGC 1589 (37.8 Mpc)						
NGC1587	Epec	1.7	-	-	0.4	-
NGC1588	Epec	1.4	-	-	0.8	-
NGC1589$^+$(c)	Sab	3.2	5.66	1.11	11.9	H
UGC03072$^+$	Im	1.3	6.37	0.58	12.8	A
UGC03058	Sm	1.3	6.77	0.18	17.6	H
NGC1593	S0	1.6	6.44	-	22.2	-
UGC03080	Sc	1.9	6.88	−0.01	37.0	H
UGC03054	Sd	1.4	6.21	0.74	43.3	H
NGC1586	Sbc	1.7	6.76	0.17	58.3	H
NGC3686 (12.2 Mpc)						
NGC3607	S0	4.9	-	-	0.0	-
NGC3608	E	3.2	-	-	5.7	-
UGC06296	Sc	1.2	6.63	0.24	15.4	A
LSBCD570-04	dI	1.0	-	-	29.9	-
UGC06341	Sdm	1.0	6.80	0.15	46.0	A
UGC06324	S0	1.7	-	-	46.0	-
NGC3626	S0	2.7	-	-	48.5	-
UGC06320	S?	0.95	7.05	−0.14	51.4	A
NGC3592	Sc	1.8	6.41	0.46	59.2	A
LSBCD570-03	dI	0.8	-	-	93.7	-
NGC3659	SBm	2.1	7.03	−0.08	98.9	A

Galaxy	*MT*	$d_l(')$	*SMD*	$def_{\rm H_I}$	Ang.	Tel.
NGC3686 (12.2 Mpc) continued						
UGC6300	E	1.2	-	-	103.8	-
NGC3655	Sc	1.5	7.11	−0.24	123.0	G
LSBCD570-02	Im	0.39	6.52	0.43	130.0	A
LSBCD570-01	Sm	0.5	6.85	0.10	137.7	A
UGC06171	IBm	2.5	6.83	0.12	142.0	RC3
NGC3681	Sbc	2.5	7.24	−0.31	154.8	G
UGC06181	Im	1.0	7.02	−0.07	157.5	G
NGC3684	Sbc	3.1	7.02	−0.09	159.4	N91
NGC3686	Sbc	3.2	6.59	0.34	162.7	N91
NGC3691	SBb	1.3	6.82	0.09	174.8	A
NGC 4261 (21 Mpc)						
NGC4261	E	4.1	-	-	0.1	-
VCC0344	E	.34	-	-	1.9	-
IC3155	S0	1.17	-	-	12.0	-
VCC0292	dE	0.35	-	-	13.0	-
NGC4269	S0+	1.1	-	-	13.0	-
VCC0388	dE	0.51	-	-	14.9	-
NGC4260	Sa	3.34	5.87	0.89	16.3	B
VCC0405	dE	.18	-	-	17.1	-
NGC4287	S	1.82	6.17	0.74	23.9	H
VCC0332	S0	0.29	-	-	28.9	-
NGC4277	S0/a	1.13	-	-	30.8	-
VCC287	dE	0.51	-	-	37.3	-
VCC0223	BCD?	0.2	7.68	−0.54	49.1	A
VCC0297	Sc	1.01	6.79	0.08	54.1	H
VCC238	dE	0.25	-	-	59.3	-
NGC4223	S0	2.6	-	-	59.5	-
HARO06	E	0.49	-	-	61.1	-
NGC4215	S0	1.9	-	-	62.3	-
NGC4255	S0	1.3	-	-	62.8	-
UGC07411	S0/a	1.4	-	-	70.7	-
NGC4197$^+$(c)	Sc	4.26	6.36	0.51	70.9	H
VCC0114$^+$	Im	0.6	7.21	−0.26	72.3	A
NGC4292	S0	1.7	-	-	79.0	-
VCC0693	S?	1.0	6.71	0.20	79.7	A
VCC0256	S	0.70	-	-	84.4	-
VCC0172	Im	1.08	7.02	−0.07	86.8	B
VCC764	S0	0.54	-	-	90.2	-
VCC468	BCD	0.3	7.25	−0.11	108.9	A
NGC4233	S0	2.4		-	-113.0	-
NGC4180	Sab	1.6	6.61	0.15	119.3	A

Galaxy	*MT*	$d_l(')$	*SMD*	$def_{\mathrm{H_I}}$	Ang.	Tel.
NGC 4589 (16.7 Mpc)						
NGC4319	Sab	3.0	-	-	11.2	ND
NGC4386	S0	2.5	-	-	11.8	-
NGC4291	E	1.9	-	-	16.8	-
NGC4363	Sb	1.4	6.90	0.01	23.3	B
NGC4331	Im	2.2	6.86	0.08	51.0	G
UGC07189	Sdm	1.7	6.70	0.25	60.5	B
UGC07265	Sdm	1.0	7.14	−0.19	64.7	G
UGC07238	Scd	1.53	6.71	0.24	65.3	B
UGC07872	Im	1.6	6.81	0.13	65.4	B
NGC4133	Sb	1.8	6.65	0.26	66.2	N91
NGC4159	Sdm	1.3	7.06	−0.11	69.8	B
NGC4589	E	3.2	-	-	84.8	-
NGC4648	E	2.1	-	-	86.2	-
NGC4127	Sc	2.5	6.97	−0.10	106.0	RC3
UGC7844	Sd	1.27	-	-	116.3	X
UGC7908	Scd	1.5	6.38	0.57	128.1	G
UGC7086	Sb	2.69	6.74	0.16	146.0	G
NGC 5044 (26.0 Mpc)						
NGC5044	E	3.0	-	-	0.5	
NGC5044-1[c]	dE	0.4	-	-	5.3	
NGC5049	S0	1.9	-	-	8.0	
LEDA083813	dE	0.4	-	-	19.0	
NGC5030	S0	1.8	-	-	23.0	
MCG-03-34-041	Sc	2.3	6.27	0.60	25.3	H
NGC5031	S0	1.6	-	-	25.3	-
LEDA083798	Sd	0.6	-	-	28.5	-
LCSBS1851O	dS0	0.7	-	-	32.6	-
MCG-03-34-020	E	0.6	-	-	35.5	-
NGC5017	E	1.8	-	-	43.0	-
IC0863	Sa	1.8	6.63	0.13	58.1	H
UGCA338	Sdm	2.0	6.86	0.09	63.1	H
MCG-03-34-014	Sc	2.5	6.67	0.20	80.6	H
MCG-03-34-004	S0	1.9	-	-	83.0	-
SGC1317.2-1702	Sdm	1.9	6.44	0.50	85.2	H
SGC1316.2-1722	Sm	2.0	6.46	0.49	90.4	H

UGC12064 (50.2 Mpc)						
UGC12064(c)	S0	1.1	-	-	0.2	-
UGC12073(c)	Sb	2.1	6.73	0.18	16.3	G
UGC12075(c)	Scd	1.4	6.77	0.18	19.1	G
UGC12077(c)	S	1.0	6.95	−0.04	33.8	G
UGC12079(c)	Dwarf	1.0	6.99	−0.04	34.0	G
IC 1459 (17.8 Mpc)						
IC1459	E	5.2	-	-	0.1	-
IC5264^{+}(c)	Sab	2.5	6.37	0.40	6.6	P
IC5269B	Scd	4.1	6.43	0.52	14.3	H
IC5269(c)	S..	1.8	7.0	−0.08	26.9	H
NGC7418	Scd	3.5	6.69	0.26	34.9	H
IC5270(c)	Sc	3.2	6.94	−0.08	37.2	H
NGC7421	Sbc	2.0	6.36	0.57	53.3	H
ESO406-G031	Sb	1.5	-	-	64.1	ND
IC5269C	Sd	2.1	6.53	0.42	79.0	H
NGC7619 (37.2 Mpc)						
NGC7619	E	2.5	-	-	0.1	-
NGC7626	E	1.3	-	-	6.8	-
UGC12510	E	1.3	-	-	9.4	-
NGC7623	S0	1.2	-	-	11.9	-
NGC7611	S0	1.5	-	-	12.8	-
KUG2318+078	S?	1.1	6.82	0.09	14.1	A
KUG2318+079B	Sc	0.3	-	-	16.2	X
NGC7608	S?	1.5	6.49	0.42	17.0	A
NGC7631	Sb	1.8	6.64	0.27	17.8	A
NGC7612	S0	1.6	-	-	23.4	-
UGC12497	Im	1.2	6.90	0.05	34.1	A
NGC7634	S0	1.2	-	-	46.1	-
CGCG406-086	S	1.3	6.56	0.35	51.5	A
FGC284A	Sc	1.12	-	-	51.7	X
UGC12480	Im	.98	7.00	−0.06	54.0	A
NGC7604	E	0.3	-	-	58.6	-
UGC12561	Sdm	1.4	6.74	0.20	62.1	A
UGC12585	Sdm	1.7	6.67	0.27	66.8	A

Blue compact dwarfs in NGC4261 group are denoted by BCD for their morphological type and are taken to belong to the category of peculiars.

[a] 2MASXJ01535632-1350125, [b] 2MASXJ01524752-1416211,

[c] NGC5044 GROUP:[FS90] 076; [+] Please see Table 4 footnote.

Table 2.4: Details of the galaxies in groups without diffuse X-ray emission

Galaxy	*MT*	$d_l(')$	*SMD*	$def_{\mathrm{H_I}}$	Ang.	Tel.
NGC 584 (18.7 Mpc)						
NGC596	E+pec	3.2	-	-	7.3	-
NGC600	Sd	3.3	6.77	0.18	17.9	H
NGC586	Sa	1.6	-	-	27.1	ND
KDG007(c)	Dwarf	1.6	6.47	0.48	29.1	H
NGC584	E	4.2	-	-	31.3	-
NGC615(c)	Sb	3.6	6.43	0.48	32.2	H
IC0127	Sb	1.8	-	-	53.1	ND
NGC636	E	2.8	-	-	90.5	-
UGCA017	Sc	2.9	6.56	0.31	119.8	H
NGC628 (7.4 Mpc)						
NGC628	Sc	10.5	7.22	-0.35	44.7	GRA
UGC1171	Im	1.3	6.39	0.55	47.4	A
UGC1176	Im	4.6	6.61	0.33	50.3	G
KDG010	Dwarf	1.5	-	-	80.8	X
IC0148	Im	2.95	7.98	−1.03	92.1	G
NGC0660	Sa	8.3	6.80	−0.03	113.2	N91
UGC01200	Im	1.5	7.06	−0.11	136.5	A
UGC01104	Im	1.0	7.50	−0.55	206.0	G
UGC01246	Im	1.5	6.96	−0.01	207.5	A
UGC01175	Sm	1.1	7.55	−0.60	245.5	G
NGC 841 (45.1 Mpc)						
NGC845	Sb	1.7	6.54	0.37	12.3	N
UGC1721	Sbc	2.0	6.97	−0.04	20.6	A
NGC841	Sab	1.8	6.78	−0.01	23.0	A
NGC834	S?	1.1	6.93	−0.02	25.5	A
UGC1673	S?	1.0	-	-	28.7	X
UGC1650	Sd	2.13	6.56	0.38	48.7	A
IC1954 (9.2 Mpc)						
NGC1311	Sm	3.0	6.59	0.35	31.5	H
IC1933	Sd	2.2	7.08	−0.13	39.3	H
IC1954	Sc	3.2	6.68	0.19	76.0	H
ESO200-G045	Im	2.0	6.26	0.69	116.0	H
NGC1249	Sdm	4.9	6.90	0.05	139.8	H
IC1959	Sm	2.8	6.89	0.06	141.1	H
NGC 1519 (18.8 Mpc)						
NGC1519^{+}(c)	Sb	2.1	6.22	0.69	4.2	H
UGCA088^{+}	Sdm	1.9	6.86	0.09	13.7	G
UGCA087	Sm	2.3	6.72	0.23	49.4	H
SGC0401.3-1720	Im	1.7	6.80	0.15	65.3	H
MCG-03-11-018	Sm	1.4	6.64	0.31	70.8	H
MCG-03-11-019	Sdm	1.6	6.98	−0.03	118.3	N

Galaxy	*MT*	$d_l(')$	*SMD*	$def_{\mathrm{H_I}}$	Ang.	Tel.
NGC 1792 (11.8 Mpc)						
NGC1808	Sb	6.5	6.58	0.33	0.0	H
NGC1792	Sbc	5.2	6.47	0.46	40.5	H
NGC1827	Scd	3.0	6.75	0.20	43.6	H
ESO305-G009	Sdm	3.5	7.03	−0.08	48.1	H
ESO362-G011	Sbc	4.5	6.77	0.16	109.5	H
ESO362-G016	Dwarf	1.3	6.71	0.23	140.6	H
ESO362-G019	Sm	2.2	6.83	0.12	163.0	H
NGC 2997 (10.6 Mpc)						
ESO434-G030	S(r)	1.0	-	-	8.2	ND
IC2507(c)	Im	1.7	7.08	−0.13	18.3	H
UGCA180(c)	Sm	2.1	7.08	−0.13	21.6	H
NGC2997	Sc	8.9	6.63	0.24	29.7	H
UGCA177	Im	1.1	6.94	0.01	38.8	H
ESO434-G041	Im	1.8	6.96	−0.01	49.2	H
ESO434-G019	Im	1.3	6.60	0.35	58.8	H
ESO373-G020	Im	1.6	6.98	−0.03	73.3	H
UGCA182	Im	2.7	6.82	0.13	73.5	H
ESO434-G039	Sa-b	1.0	6.82	−0.05	79.3	H
ESO434-G017	dwarf	1.2	6.74	0.21	88.4	H
UGCA168	Scd	5.8	6.54	0.41	161.7	H
ESO373-G007	Im	1.3	6.77	0.18	175.2	H
NGC3264 (9.8 Mpc)						
NGC3264	Sdm	2.9	6.87	0.08	22.5	G
UGCA211	pec	0.56	7.43	−0.29	33.6	G
NGC3220	Sb	1.23	7.04	−0.13	70.0	N
NGC3206	Scd	2.2	7.31	−0.36	81.8	N91
UGC05848	Sm	1.45	6.99	−0.05	111.4	G
NGC3353	BCD/Irr	1.2	7.35	−0.21	123.3	N43
NGC 4487 (10.1 Mpc)						
NGC4504	Scd	4.4	7.06	−0.11	29.9	H
UGCA289	Sdm	4.1	6.54	0.41	35.0	H
NGC4487	Scd	4.2	6.58	0.36	60.4	H
NGC4597	Sm	4.1	6.84	0.11	131.9	H
NGC 5061 (20.8 Mpc)						
NGC5061	E	3.5	-	-	12.1	-
NGC5078(c)	Sa	4.0	6.49	0.27	33.1	H
ESO508-G039	Sm	1.3	6.84	0.11	33.1	H
IC0879(c)	Sab pec	1.2	6.49	0.27	33.5	H
IC874	S0	1.2	-	-	44.1	-
NGC5101	S0/a	5.4	-	-	49.5	-
ESO508-G051	Sdm	1.4	6.90	0.05	52.8	H
IC4231	Sbc	1.7	6.72	0.21	67.5	H
ESO508-G059	S..	1.2	-	-	93.0	ND
ESO508-G034	Sm	1.2	7.40	−0.45	97.2	H

Galaxy	*MT*	$d_l(')$	*SMD*	$def_{\mathrm{H_I}}$	Ang.	Tel.
NGC 5907 (7.4 Mpc)						
NGC5907	Sc	12.77	6.65	0.22	6.7	G
UGC09776	Im	0.8	7.27	−0.32	42.7	G
NGC5866B	Sdm	1.46	7.30	−0.35	52.1	G
NGC5879	Sbc	3.74	6.80	0.12	64.7	N91
NGC5866	S0	4.7	-	-	91.7	-
UGC 9858 (25.2 Mpc)						
UGC09856	Sc	2.26	6.45	0.42	12.0	G
UGC09858	Sbc	4.3	6.79	0.14	32.0	N91
NGC5929(c)	Sab	1.0	6.31	0.45	34.7	G
NGC5930(c)	Sb	1.7	6.45	0.46	35.0	G
UGC09857(c)	Im	1.6	6.49	0.46	38.0	G
NGC 6949 (26.6 Mpc)						
NGC6949	S	1.4	7.40	−0.49	40.7	G
UGC11613	Sdm	1.85	6.87	0.08	46.0	G
UGC11636	Scd	1.3	7.03	−0.08	49.2	G
NGC 7448 (21.3 Mpc)						
NGC 7464	E	0.8	-	-	13.3	-
NGC 7465	S0	1.2	-	-	14.7	-
UGC 12313	Im	1.4	7.08	−0.13	15.2	A
NGC 7448	Sbc	2.7	7.08	−0.15	16.2	A
UGC 12321	Sbc	1.0	7.14	−0.21	20.2	A
NGC 7454	E	2.2	-	-	30.8	-
NGC 7468	E	0.9	-	-	52.0	-
UGC 12350	Sm	2.6	6.89	0.06	85.6	A
NGC 7582 (16.1 Mpc)						
ESO291-G015*(c)	Sa	1.3	6.21	0.56	3.3	H
NGC7582*(c)	Sab	5.0	6.42	0.35	9.0	H
NGC7590*(c)	Sbc	2.7	6.57	0.36	18.3	H
NGC7599*(c)	Sc	4.4	6.51	0.36	19.9	H
NGC7552	Sab	3.4	6.81	−0.04	23.3	H
NGC7632	S0	2.2	-	-	41.6	-
ESO347-G008	Sm	1.7	6.88	0.07	55.2	H
ESO291-G024	Sc pec	1.46	6.48	0.39	60.4	H
NGC7531	Sbc	4.5	6.68	0.25	75.1	H
NGC7496	Sbc	3.3	6.86	0.07	107.7	H
IC5325	Sbc	2.8	6.56	0.36	136.8	P

Galaxy	*MT*	$d_l(')$	*SMD*	$def_{\rm H\,I}$	Ang.	Tel.
NGC 7716 (27.0 Mpc)						
NGC7714(c)	Sb pec	1.9	6.73	0.18	0.0	H
NGC7715(c)	Im pec	2.6	6.77	0.18	2.0	H
UGC12690	Sm	2.0	6.65	0.30	58.1	H
UGC 12843 (17.6 Mpc)						
UGC 12843	Sdm	2.8	6.96	−0.01	8.8	A
UGC 12846	Sm	1.8	6.77	0.17	36.4	A
UGC 12856	Im	1.6	7.26	−0.31	61.5	G
MCG+03-01-003	Sm	0.45	-	-	62.0	X

Symbols used for indicating the telescopes:

A = Arecibo 1000 ft
B = Effelsberg 100 m
G = Green Bank Telescope 100 m
GRA = Agassiz Harvard 60ft
H = H I Parkes All Sky Survey
N = Nancay 30 × 300 m
N91 = NRAO 91 m
N43 = NRAO 43 m
P = Parkes 64 m

Spirals with no H I data – X; H I non detection – ND

The cases of confusion are indicated by a '(c)' in column 1.

+ HIPASS spectra towards NGC1519, NGC1589, NGC4197 and IC5264 are confused, respectively, with galaxies UGCA088, UGC03072, VCC0114 and NGC7481A. Hence, their deficiencies have been calculated following the prescription mentioned in the text. NGC7481A does not belong to the group as per the criteria and is not in the table. The other three confusing galaxies viz. UGCA088, UGC03072 and VCC0114 have GBT (the first one) or Arecibo (the last two) measurements. Therefore, their deficiencies have been calculated with the higher resolution fluxes and are not marked with a '(c)' in the above table.

* NGC7582 is confused with NGC7590 and NGC7599 in one HIPASS pointing and with ESO-291-G015 in another. Since it is closer to the pointing center in the first case, we use the deficiency calculated from that spectrum for this galaxy.